Korean J. Chem. Eng., **29**(4), 494-502 (2012)
DOI: 10.1007/s11814-011-0211-5

Adsorption characteristics of methylene blue on poplar leaf in batch mode: Equilibrium, kinetics and thermodynamics

Xiuli Han†, Xiaona Niu, and Xiaojian Ma

School of Chemical Engineering and Energy, Zhengzhou University, Kexue Road 100#, Zhengzhou, Henan 450001, P. R. China
(*Received 22 March 2011 • accepted 13 August 2011*)

Abstract−Adsorption characteristics of methylene blue (MB) from aqueous solution on natural poplar leaf were investigated. Batch experiments were carried out to study the effects of initial pH, contact time, adsorbent dosage, and initial MB concentration, salt concentration (Ca^{2+} and Na^{+}) as well as temperature on MB adsorption. The optimum condition for adsorption was found at pH 6-9 and adsorbent dosage of 2 g L^{-1}. The equilibration time was 240 min. The salt concentration had a negative effect on MB removal. The equilibrium data were analyzed with Langmuir, Freundlich and Koble-Corrigan isotherm models using nonlinear regression method. The adsorption process was more effectively described by Langmuir isotherm based on the values of the correlation coefficient R^2 and chi-square statistic x^2. The maximum monolayer adsorption capacity of poplar leaf from the Langmuir model was 135.35 mg g^{-1} at 293 K. The pseudo second order equation provided a better fit to experimental data in the kinetic studies. Intraparticle diffusion was involved in adsorption process, but it was not the only rate-controlling step. Thermodynamic quantities such as ΔG, ΔH and ΔS were calculated, indicating that the adsorption process was spontaneous and endothermic. Dye-adsorbent interactions were examined by FTIR and SEM analysis. The FTIR results suggested that there were hydroxyl and carboxyl groups on the surface of poplar leaf, which would make MB adsorption possible. The SEM images showed effective adsorption of MB molecules on the adsorbent surface.

Key words: Adsorption, Methylene Blue, Poplar Leaf, Isotherm, Kinetics, Thermodynamics

INTRODUCTION

Extensive use of synthetic dyestuffs in a number of industrial processes such as textile, paper, plastics, food, cosmetics, and leather has brought about intractable environmental problems. Even a thimbleful of dye in water is highly visible and disgusting. The presence of various dyes also causes damage to living beings in water by reducing light penetration and inhibition of photosynthesis [1]. In addition, the stability of most dye molecules under the condition of light, heat and chemicals leads to the fact that the dyeing effluents are difficult to degrade [2,3]. Economic, effective and feasible methods for comprehensive treatment of dyeing industrial effluents are therefore paid much more attention, owing to the increased environmental stress and consciousness from people.

Processing methods on dye removal are classified as coagulation, chemical oxidation, flocculation, hyper filtration, biological treatment and adsorption. Adsorption onto activated carbon has been widely used in actual effluent treatment as a highly effective process. However, the application of this material is limited due to high cost and the difficulty in regeneration [4,5]. Therefore, studies on dye removal have been focusing on searching for abundant and low-cost adsorbents. For instance, agricultural by-products such as neem sawdust [6], palm kernel fiber [7], apple pomace [1], rice husk [8,9], tree fern [10], lemon peel [11] and pineapple leaf [12] have been widely studied for dye removal.

†To whom correspondence should be addressed.
E-mail: xlhan@zzu.edu.cn

The poplar leaf powders have been reported to have the potential as a novel adsorbent for heavy metals removal [13,14]. In this work, the biomaterial was tested for its ability to adsorb alkaline dyestuff from aqueous solution. The fallen poplar leaf could be obtained easily in campuses and city streets. Methylene blue dissolved in aqueous solution was taken as the simulated industrial effluent. Investigations were made to evaluate the potential of poplar leaf for MB removal in batch system. The respective thermodynamic and kinetic studies were also carried out, and the isotherm constants for the Langmuir, Freundlich and Koble-Corrigan models were calculated by nonlinear regression analysis.

MATERIALS AND METHODS

1. Preparation of Adsorbent and MB Solution

The fallen poplar leaves were collected from Zhengzhou University in autumn. Then the materials were continuously washed with distilled water to remove the surface dirty particles. The washed leaves were dried at 80 °C in an oven for several hours until constant weight and crushed to particle sizes in the range of 20-40 mesh with a grinder (JFSD-100, China).

Methylene Blue widely used in synthetic fiber and paper industries was obtained from Zhengzhou Chemical Corporation in China. Its chemical structure is shown in Fig. 1. The molecular weight of methylene blue is 373.9 g mol^{-1}. The stock solution of MB was prepared by dissolving MB (0.2 g) into distilled water (1 L). Then the stock solution was diluted to working concentrations ranging from 20 to 200 mg L^{-1}.

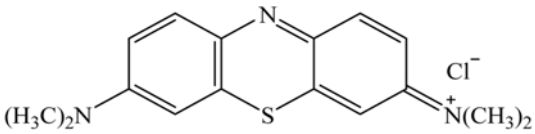

Fig. 1. The chemical structure of methylene blue.

2. Methods

Both poplar leaf and MB solution (20 mL) at the desired concentration were placed in a 50 mL conical flask. Then the conical flask was agitated at 100 rpm min^{-1} in a water bath shaker at the needed temperature to attain equilibrium. The solution and solid phase were separated by filtration with syringe filter. The filtrate was analyzed using UV-vis Spectrophotometer (WFZ UV-2102PC) for MB concentration. Percent removal efficiency (%R) and the amount of MB adsorbed on per unit mass of poplar leaf (q) were determined respectively as follows:

$$\%R = \frac{C_0 - C_f}{C_0} \times 100 \quad (1)$$

$$q = \frac{(C_0 - C_f) \times V}{m} \quad (2)$$

Where C_0 and C_f (mg L^{-1}) are the initial MB concentration and final MB concentration after adsorption, V (L) the volume of MB solution, and m (g) is the total mass of poplar leaf.

Influences of contact time, initial pH, adsorbent dosage, dye concentration, salt concentration and temperature were investigated as described above.

3. Characterization of Poplar Leaf

The presence of different functional groups present in poplar leaf was characterized with a FTIR spectrophotometer (PE-1710, USA). The poplar leaf of 0.02 g and the KBr powders were mixed adequately, and then the mixture was pressed to a flake. The FTIR spectrum was recorded by scanning of the spectrophotometer. The spectral range changed from 4,000 to 400 cm^{-1}. Scanning electron micrographs of poplar leaf were obtained by scanning electron microscopy (JEOL 6335F-SEM, Japan). Before analysis, the samples were coated with a thin layer of gold under an argon atmosphere. An element analyzer (EA1112, USA) was used to determine the major elements of poplar leaf. The point of zero charge (pH_{PZC}) of poplar leaf was measured at different pH values (2-11) at a constant electrolyte concentration of 0.01 mol L^{-1} by means of a pH-meter (pHS-3C, China). Then initial and final pH after an equilibrium time of 240 min was also measured.

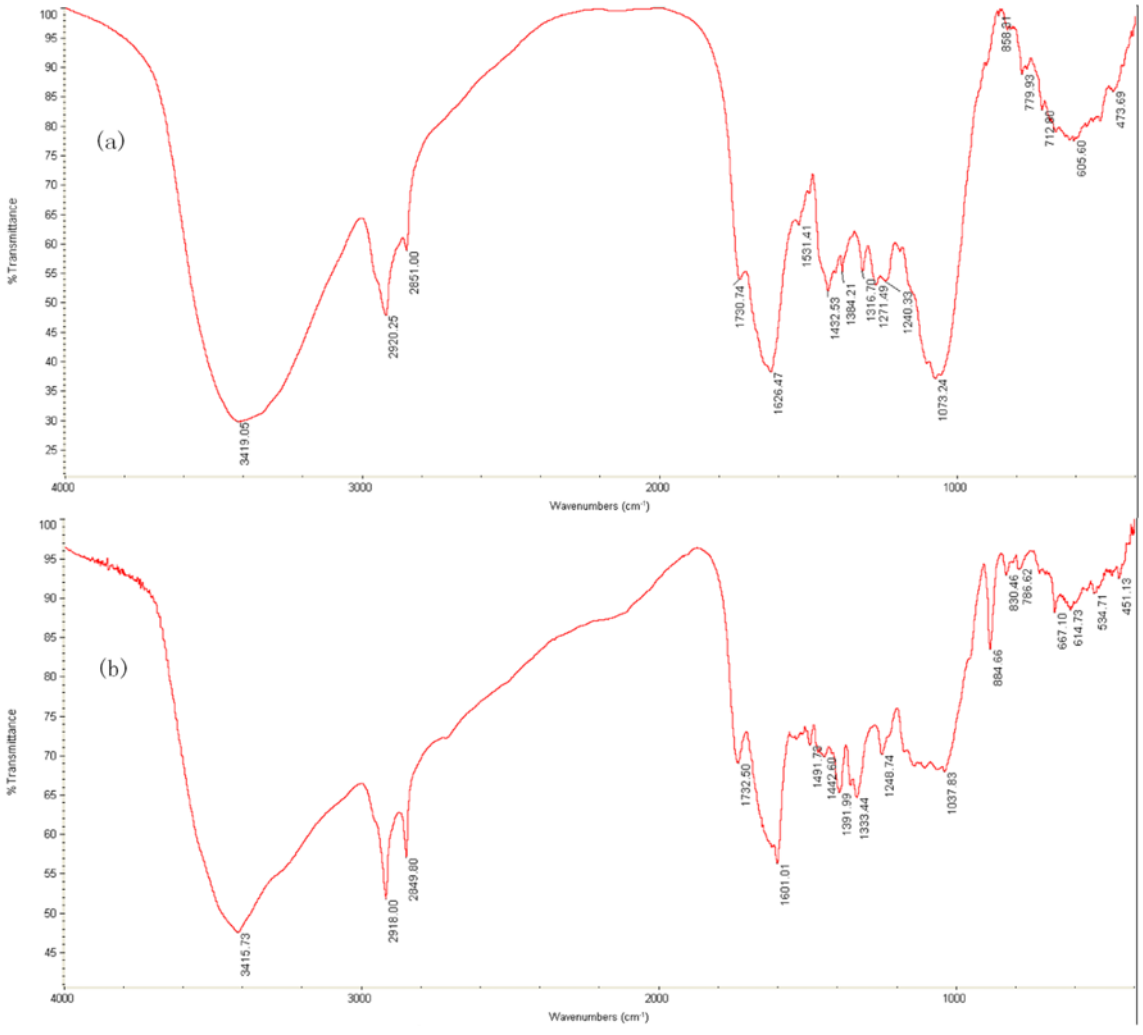

Fig. 2. FTIR spectrum of natural poplar leaf (a) and dye loaded poplar leaf (b).

RESULTS AND DISCUSSION

1. Property of Adsorbent

The FTIR analysis confirmed functional groups on the surface of poplar leaf. The infrared spectrum of poplar leaf before adsorption is presented in Fig. 2(a). The band at 3,419 cm^{-1} is associated O-H stretching vibration. The strong peak at around 1,626 cm^{-1} is caused by C=O stretching band of carboxyl groups. A 1,432 cm^{-1} is due to C-O stretching from carboxyl groups. The infrared spectrum of poplar leaf after adsorption is shown in Fig. 2(b). The band of O-H stretching vibration is slightly shifted from 3,419 to 3,415 cm^{-1}. The peaks of C=O stretching band and C-O stretching from carboxyl groups are also shifted to 1,602 cm^{-1} and 1,491 cm^{-1}, respectively.

FTIR spectrum indicated that there are large numbers of hydroxyl and carboxyl groups on the surface of poplar leaf, which possibly react with dye molecules in aqueous solution. The surface of poplar leaf is negatively charged at proper pH due to deprotonation of acid groups such as carboxyl and hydroxyl groups. These groups may be the major adsorption sites for cationic dye.

The scanning electron micrograph of original poplar leaf (Fig. 3(a)) at a magnification of 2,000 times represented highly heterogeneous surface with porous structure. The rough and porous surface conduced to an increase in surface area of poplar leaf [15]. The SEM image of poplar leaf after MB adsorption (Fig. 3(b)) shows significant differences from Fig. 3(a), indicating an effective adsorption of MB molecules onto poplar leaf [16]. The results of element analysis of poplar leaf were found to be C 43.79%, H 6.25%, N 1.54%, S 0.22%.

The pH_{PZC} is a concept related to the phenomenon of adsorption that describes the condition when the electrical charge density on the adsorbent surface is zero. The pH_{PZC} of poplar leaf was obtained from the plot of ΔpH (the difference between initial pH and final pH at equilibrium) versus initial pH. The results shown in Fig. 4 indicate that the pH_{PZC} of poplar leaf was around 5.6. The adsorbent surface was positively charged at $pH<pH_{PZC}$, and the adsor-

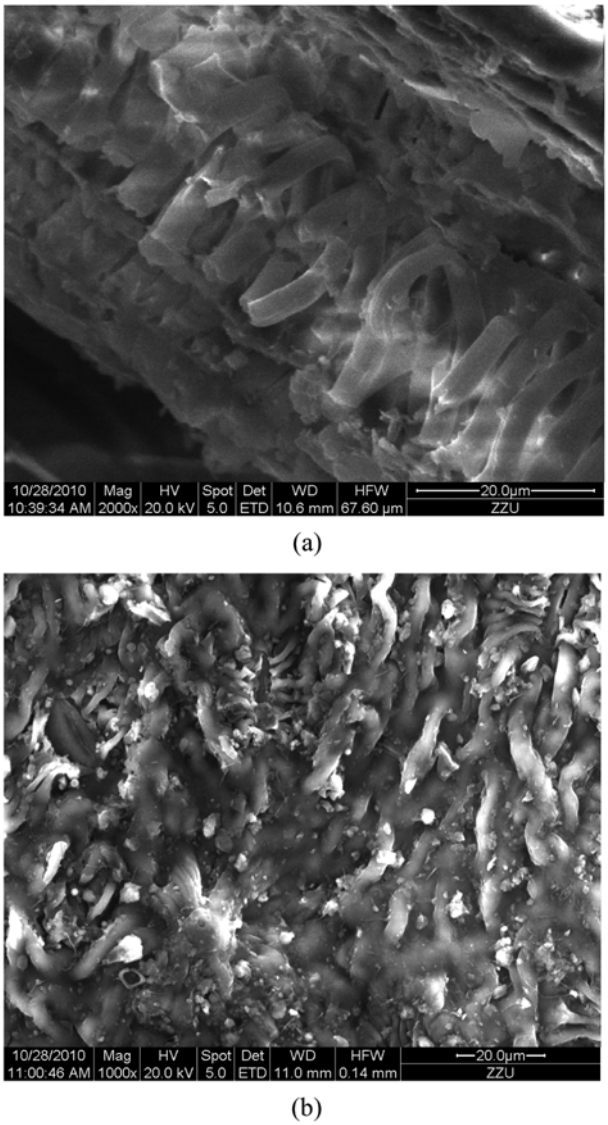

Fig. 3. SEM images: (a) natural poplar leaf and (b) poplar leaf after adsorption of MB.

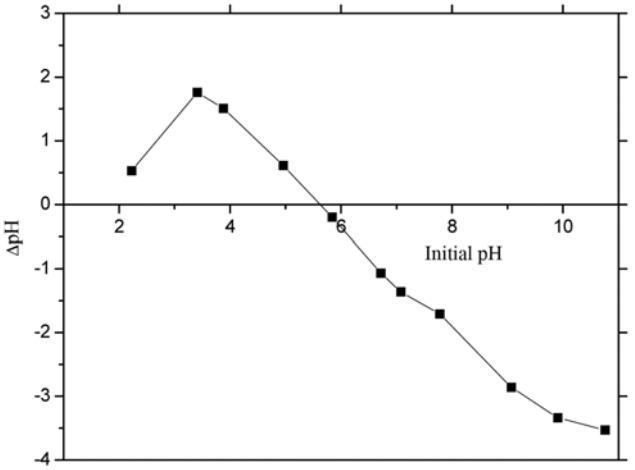

Fig. 4. The point of zero charge of poplar leaf.

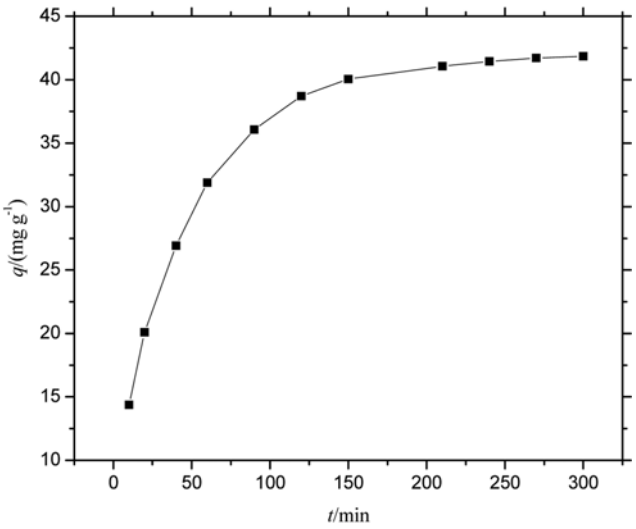

Fig. 5. Effect of contact time for the adsorption of MB on poplar leaf at 293 K (C_0=100 mg L^{-1}; V=0.01 L; adsorbent dose= 2 g L^{-1}).

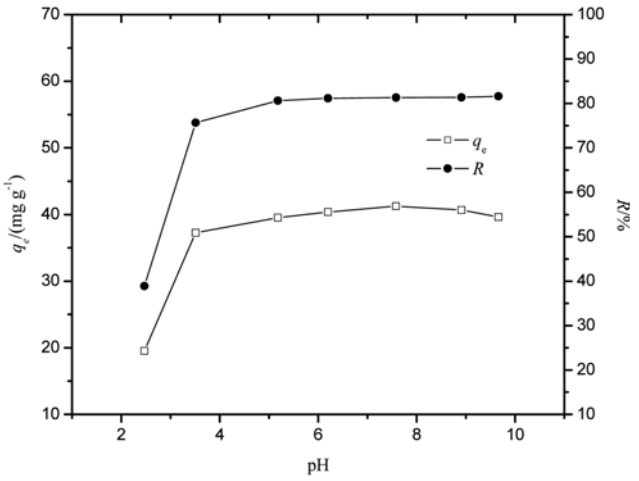

Fig. 6. Effect of initial pH for adsorption of MB on poplar leaf at 293 K (C_0=100 mg L^{-1}; V=0.01 L; adsorbent dosage=2 g L^{-1}).

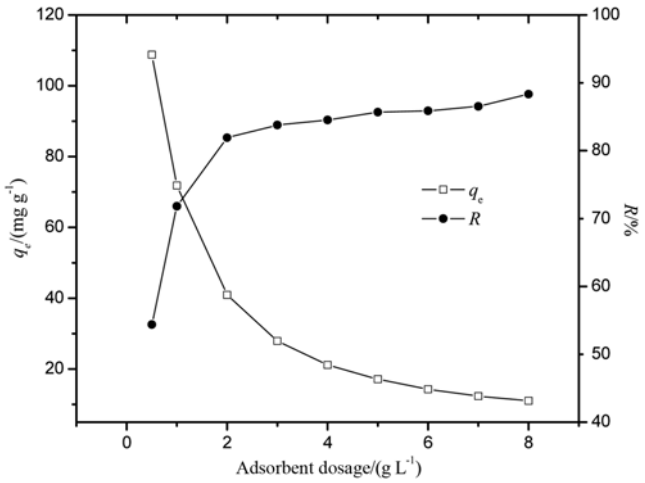

Fig. 7. Effect of adsorbent dosage for the adsorption of MB on poplar leaf at 293 K (C_0=100 mg L^{-1}; V=0.01 L).

bent presented a negative surface charge at pH>pH_{PZC}.

2. Effect of Contact Time

Experiments were performed to investigate the effect of contact time (10 to 300 min) for MB (C_0=100 mg L^{-1}) removal from aqueous solution at 293 K. In Fig. 5, MB adsorption represents a two-step kinetic process. The rate of MB adsorption on poplar leaf was rapid in the beginning, but it gradually reduced with time until the system reached equilibrium. It was evident that the amount of MB adsorbed on per unit mass of poplar leaf increased quickly in the first stage. The second stage was a much slower adsorption process after 120 min. The values of q changed slowly. So within 180 min, adsorption equilibrium was nearly established. In the following batch experiments, 240 min was taken to ensure equilibrium.

3. Effect of Initial pH

Initial pH of dye solution has an effect on the property of surface charge, which plays an important role in dye removal. Fig. 6 shows the effect of solution pH (2-10) for MB removal. The solution pH was adjusted with 0.1 mol L^{-1} HCl and 0.1 mol L^{-1} NaOH. The dye adsorption on poplar leaf was significantly affected over the pH range of 2-4. It was observed that the values of %R increased from 38% to nearly 80% and the adsorption quantity increased from 20 to 40 mg g^{-1} when the value of pH increased from 2 to 4. The results, however, show the constant MB adsorption when initial solution pH varied from 5 to 10. The values of %R and adsorption quantity were approximately unchanged.

It may be explained that at low pH, active groups on the surface of poplar leaf such as carboxyl, hydroxyl groups were more protonated, and positive charges surrounded the surface of adsorbent. The phenomenon hindered the adsorption of basic dye due to competition for adsorption sites between dye cations and protons. When the initial pH increased, the active groups on the surface of adsorbent may have become negatively charged, which provided more binding sites for the positively charged dye cations due to electrostatic attraction [1,9]. The results of solution pH experiments agreed with the adsorbent surface property represented from FTIR analysis and pH_{PZC} measurement. We concluded that the higher pH (6-9) favored MB removal on poplar leaf in practice. The pH of original solution was near 7, and it was not adjusted in subsequent batch experiments. The adsorption mechanism explained that poplar leaf was favorable to remove basic dye.

4. Effect of Adsorbent Dosage

The plot of adsorption capacity and percent removal efficiency versus the adsorbent dosage at initial MB concentration of 100 mg L^{-1} is shown in Fig. 7. The percent removal efficiency increased from 54.4% to 88.3% as the adsorbent dosage increased from 0.5 to 8 g L^{-1}, while the adsorption capacity q_e decreased from 108.7 to 11.04 mg g^{-1} with an increase in adsorbent dosage. At higher adsorbent dosage, many more adsorption sites were available and adsorption surface area was increased, which contributed to an increase of MB amount adsorbed on adsorbents [7]. However, there was a very fast superficial adsorption onto the poplar leaf surface at higher adsorbent dosage, which produced a lower solute concentration in the solution than when the poplar leaf dosage was lower. Splitting effects of concentration gradient caused a decrease in q_e [17-19].

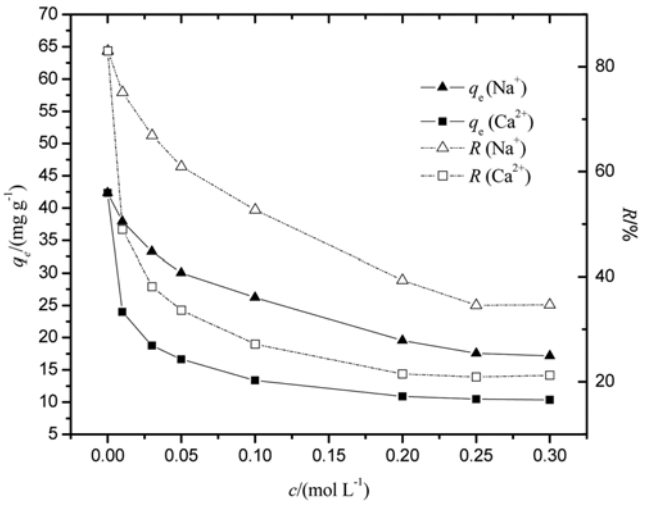

Fig. 8. Effect of salt concentration for adsorption of MB on poplar leaf at 293 K (C_0=100 mg L^{-1}; V=0.01 L; adsorbent dosage=2 g L^{-1}).

The optimum adsorbent dosage was taken as 2 g L^{-1} for this study on MB removal.

5. Effect of Salt Concentration (NaCl and $CaCl_2$)

It is essential to investigate the effect of salt concentration (NaCl and $CaCl_2$) for dye removal because of the presence of salt ions in actual dyestuff effluents. This experiment was carried out by dissolving calculated mass of NaCl and $CaCl_2$ into MB solution of 0.01 L. It was observed from Fig. 8 that both Na^+ and Ca^{2+} had negative effects on MB removal. The adsorption capacity decreased from 42.36 to 10.36 mg g^{-1}, and the percent removal efficiency decreased from 83.03% to 21.24% with an increase in Ca^{2+} concentration from 0 to 0.3 mol L^{-1}. The values of q_e decreased from 42.36 to 17.17 mg g^{-1}, and the percent removal efficiency decreased from 83.03% to 34.68% by increasing Na^+ concentration from 0 to 0.3 mol L^{-1}.

The possible reason for the negative effect was that Na^+ and Ca^{2+} competed with dye cations for active sites on the surface of adsorbent. As Ca^{2+} had more contribution to ionic strength and more positive charge than Na^+, the effect of Ca^{2+} on adsorption was stronger than Na^+ in the same mole concentration [20,21].

6. Effect of Temperature and Initial MB Concentration

Removal of MB by poplar leaf was performed by varying dye concentration from 20 to 200 mg L^{-1} at temperature 293, 303 and 313 K, respectively. Fig. 9 shows that adsorption capacity on per unit weight of adsorbent increased from 8.43 to 69.43 mg g^{-1} at 293 K, from 8.51 to 70.49 mg g^{-1} at 303 K, and from 8.62 to 71.4 mg g^{-1} at 313 K by increasing MB concentration. At the same temperature, the increased initial MB concentration resulted in a higher driving force for mass transfer due to the fact that active sites on poplar leaf were surrounded by more MB cations when initial MB concentration was high [22]. Hence, a higher initial MB concentration favored the adsorption process.

Adsorption of MB on poplar leaf was enhanced by increasing the temperature from 293 to 313 K at different initial dye concentration. According to Fig. 9, there was a slight increase in equilibrium adsorption capacity at the same dye concentration when temperature was higher. The effect was attributed to an endothermic process. Similar results have been reported by Bulut et al. [23] for MB adsorption onto wheat shells and Kumar et al. [24] for MB adsorption onto mango seed kernel powder. To investigate the effect of temperature on MB adsorption, thermodynamic parameters were determined.

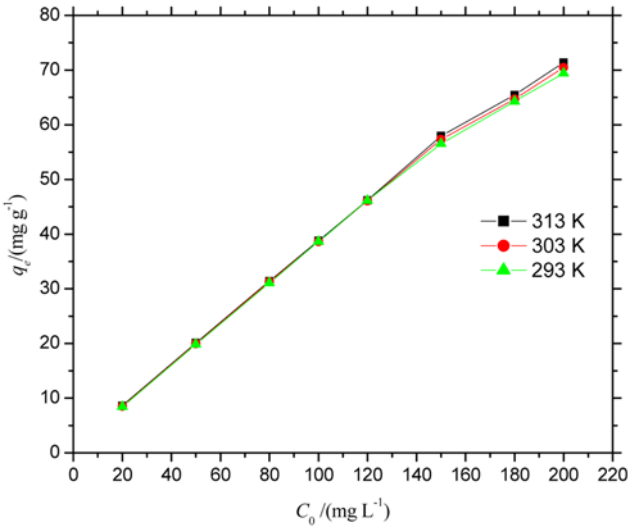

Fig. 9. Effect of initial dye concentration and temperature for adsorption of MB on poplar leaf (V=0.01 L; adsorbent dosage=2 g L^{-1}).

Table 1. Thermodynamic parameter in the system of MB biosorption

Temperature	K	ΔG (kJ mol^{-1})	ΔH (kJ mol^{-1})	ΔS (kJ mol^{-1} K^{-1})
293 K	5.37	−4.095	-	-
303 K	5.71	−4.389	5.6008	0.0331
313 K	6.22	−4.756	-	-

7. Thermodynamic Study for MB Removal

Thermodynamic parameters indicate energy transformation in the adsorption process, which can estimate the effect of temperature for MB removal. Thermodynamic parameters, standard free energy change (ΔG), enthalpy change (ΔH) and entropy change (ΔS) at different temperature were calculated by the following normal equations:

$$\Delta G = -RT\ln K = \Delta H - T\Delta S \quad (3)$$

$$\ln K = -\frac{\Delta G}{RT} = -\frac{\Delta H}{RT} + \frac{\Delta S}{R} \quad (4)$$

Where equilibrium constant K was obtained from linear form of the Langmuir equation [25], R the universal gas constant (8.314 J mol^{-1} K^{-1}), and T (K) the temperature of MB/poplar leaf system.

The calculated thermodynamic parameters are listed in Table 1. The standard free energy change in the adsorption system was −4.095, −4.389 and −4.756 kJ mol^{-1} at temperature 293, 303 and 313 K, respectively. The negative value of ΔG indicated a spontaneous process for MB adsorption onto poplar leaf. Experimental results illustrated that as temperature increased, MB adsorption was much more favorable according to the positive value of ΔH (5.6008 kJ mol^{-1}) in Table 1. This result proved endothermic reaction for adsorption process. More energy was required to improve adsorption capacity at a certain range of temperature. Entropy change (ΔS) was 0.0331 kJ mol^{-1} K^{-1}, corresponding to an increase of freedom of the adsorbed species during the surface reaction [12]. The value of ΔS was low, which indicated no remarkable change on entropy emerging.

8. Adsorption Equilibrium

From equilibrium data in Fig. 9, the relation between initial dye concentration C_0 and adsorption capacity q_e was considered as linearity apparently. Equilibrium data at different temperature were analyzed using linear regression method. The slope of the fitted line in Table 2 became larger with an increase in temperature. The high values of R^2 (R^2>0.997) proved the linear relation for plot of q_e versus

Table 2. The relationship between adsorption capacity at equilibrium (q_e) and initial dye concentration (C_0)

T	293 K	303 K	313 K
Adsorption expression	q_e=0.342C_0	q_e=0.347C_0	q_e=0.352C_0
R^2	0.998	0.998	0.997

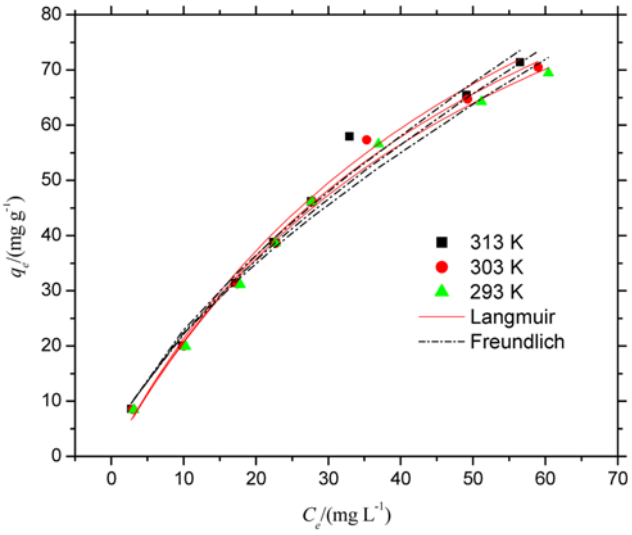

Fig. 10. Adsorption isotherm curves fitted with Langmuir and Freundlich models.

C_0 within the range of experimental dye concentration.

The equilibrium adsorption isotherm is most important in investigating adsorption mechanism. Surface property, adsorption affinity of adsorbent and the maximum adsorption capacity can be obtained from the adsorption isotherm and correlative constants. In this study, experimental adsorption equilibrium data obtained at 293, 303 and 313 K were fitted by nonlinear regression method with Langmuir and Freundlich models. The fitted curves with the two well-known isotherm models are shown in Fig. 10.

Langmuir isotherm equation is described as:

$$q_e = \frac{q_m a_L C_e}{1 + a_L C_e} \quad (5)$$

where a_L is Langmuir equilibrium constant related to binding energy of adsorption, and q_m is the maximum monolayer adsorption capacity based on hypothesis of homogeneous surface for adsorption. The calculated values of a_L, q_m, nonlinear chi-square statistic x^2 and nonlinear regression coefficient R^2 at different temperature are given in Table 3. The uncertainties of some parameters are also presented in Table 3. It was seen that the maximum monolayer capacity of poplar leaf is determined as 135.35, 142.77 and 147.42 mg g^{-1} for 293, 303 and 313 K. The values of q_m increased slightly on increasing the temperature, while equilibrium constant a_L decreased as temperature increased. Nonlinear regression coefficients R^2 were all above 0.985. Chi-square analysis was also used as an evaluating indicator for Langmuir model, which indicated that the Langmuir model fits were quite well for experimental data.

Table 4. Comparison of adsorption capacity of methylene blue with various biosorbents

q_m (mg g^{-1})	Biosorbents	References
135.4	Poplar leaf	This paper
72.1	Peanut husk	[26]
80.9	Phoenix leaf	[21]
185.2	Brazilian pine-fruit shell	[27]
221.7	Lotus leaf	[28]

A comparison of adsorption capacity q_m of methylene blue on various biosorbents is listed in Table 4. It was evident from the published literature that poplar leaf has a lower adsorption capacity on MB compared with Brazilian pine-fruit shell and lotus leaf, and a higher adsorption capacity compared to peanut husk and phoenix leaf. In addition, poplar leaves are abundant and cheap. There is a huge potential to use poplar leaf for the adsorption of MB molecules from industrial effluents.

The Freundlich isotherm equation is defined as follows:

$$q_e = K_F C_e^{1/n} \quad (6)$$

Where K_F and 1/n are Freundlich constants. K_F is related to the af-

Table 3. Langmuir, Freundlich and Koble-Corrigan isotherm parameters for MB adsorption onto fallen poplar leaf at different temperatures using nonlinear regressive method

	293 K	303 K	313 K
Langmuir			
a_L (L mg^{-1})	0.0179±0.00216	0.0170±0.00252	0.0169±0.00342
q_m (mg g^{-1})	135.35±9.620	142.77±12.805	147.42±18.348
R^2	0.995	0.993	0.988
x^2	2.61	3.71	6.83
Freundlich			
K_F [mg g^{-1} (L mg^{-1})$^{1/n}$]	4.883±0.784	4.791±0.783	4.827±0.898
1/n	0.657±0.043	0.669±0.044	0.675±0.051
R^2	0.985	0.985	0.981
x^2	7.95	8.18	10.72
Koble-Corrigan			
A	1.915±0.653	2.106±0.848	2.237±1.216
B	0.01629±0.0033	0.01626±0.0035	0.01638±0.0045
n	1.098±0.138	1.0603±0.165	1.045±0.226
R^2	0.996	0.993	0.988
x^2	2.86	4.35	8.14

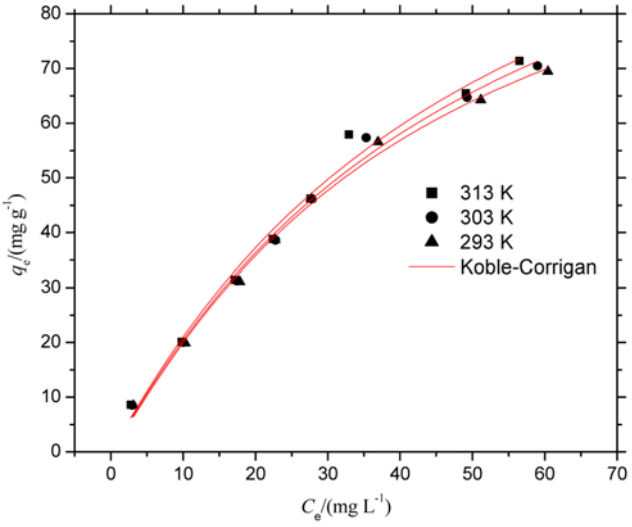

Fig. 11. Adsorption isotherm curves fitted with Koble-Corrigan model.

finity and the adsorption capacity of adsorbent and 1/n is related to the surface heterogeneity. The calculated 1/n ($0.1<1/n<1$) represents an isotherm curve form which indicates powerful adsorption attraction between solid phase and liquid phase in the adsorption system [29]. The magnitude of R^2 and x^2 indicated the fit of the data to Freundlich equation, which meant the heterogeneous surface of poplar leaf [30]. Based on a comparison of values of R^2 and x^2, the adsorption isotherms were better described by the Langmuir equation.

A three-parameter isotherm equation, Koble-Corrigan, was used to analyze equilibrium data, and expressed as:

$$q_e = \frac{AC_e^n}{1+BC_e^n} \tag{7}$$

Where A, B, n are Koble-Corrigan parameters. The Koble-Corrigan model is a combination of Langmuir and Freundlich model. The fitted curves are shown in Fig. 11 and the values of related parameters are listed in Table 3. The values of parameter n are close to 1, which indicates that the isotherms are approaching more of the Langmuir form. The values of A increased and parameter B kept unchanged with temperature changing from 293 to 303 K. The Koble-Corrigan model was suitable for experimental data well based on values of nonlinear regression coefficient R^2 ($R^2>0.988$) and x^2 ($x^2<8.14$), which suggested that equilibrium data conformed to Freundlich isotherm at low dye concentration and followed Langmuir model at higher dye concentration [31].

9. Adsorption Kinetics

Adsorption rate constants and intraparticle diffusion mechanism were investigated using the pseudo first-order kinetic model, pseudo second-order kinetic model and intraparticle diffusion equation by linear regression method, respectively.

The pseudo first-order kinetic model is expressed as:

$$\log(q_e - q_t) = \log q_{e1} - \frac{k_1 t}{2.303} \tag{8}$$

Where q_e and q_t (mg g^{-1}) are adsorption capacity on per unit dose of adsorbent at equilibrium and at time t (min), q_{e1} the predicted values of q_e from pseudo first-order kinetic model and k_1 (min^{-1}) the first-order rate constant. The plot of $\log(q_e - q_t)$ versus t is linear. The rate constant k_1 is calculated from the slope of the plot.

The pseudo second-order kinetic equation is

$$\frac{t}{q_t} = \frac{1}{k_2 q_{e2}^2} + \frac{t}{q_{e2}} \tag{9}$$

Where k_2 (g mg^{-1} min^{-1}) is the pseudo second-order rate constant and q_{e2} (mg g^{-1}) is the calculated value of adsorption capacity at equilibrium according to pseudo second-order kinetic equation. The values of k_2 and q_{e2} were obtained from the plot of t/q_t against t.

Fig. 12 and Fig. 13 show the fitted curves with the pseudo first- and second-order model. The pseudo second-order kinetic model shows a better fit to the whole range of contact time due to higher value of correlation coefficient R^2 and lower value of standard deviation (SD) listed in Table 5. Moreover, the predicted q_e from pseudo

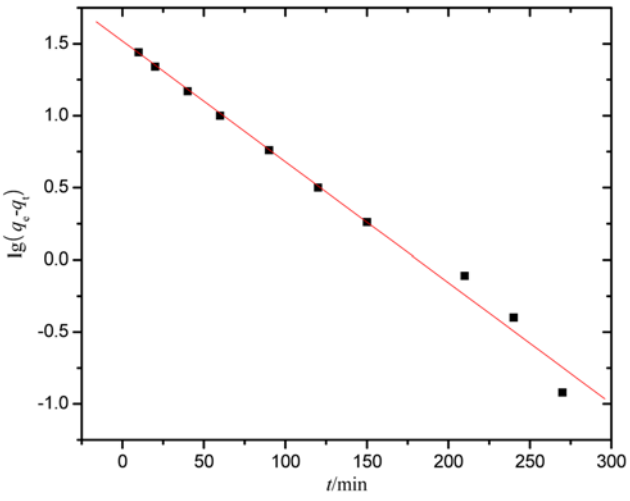

Fig. 12. Pseudo first order kinetic plot for adsorption of MB on poplar leaf at 293 K.

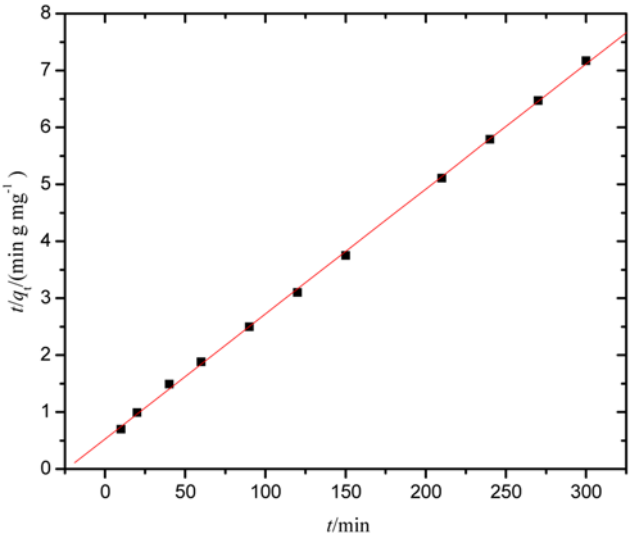

Fig. 13. Pseudo second order kinetic plot for adsorption of MB on poplar leaf at 293 K.

Table 5. Kinetic parameters for adsorption of MB on natural poplar leaves at 293 K

Model		Parameter 1		Parameter 2	R^2	SD
Pseudo first order	k_1	0.0193 min^{-1}	q_{e1}	33.06 mg g^{-1}	0.995	0.0848
Pseudo second order	k_2	9.17E-4 g mg^{-1} min^{-1}	q_{e2}	45.54 mg g^{-1}	1.000	0.0518
Intraparticle diffusion	k_{i1}	3.45 mg g^{-1} $min^{-1/2}$	C_1	4.33 mg g^{-1}	0.995	1.021
	k_{i2}	0.37 mg g^{-1} $min^{-1/2}$	C_2	35.67 mg g^{-1}	0.985	0.144

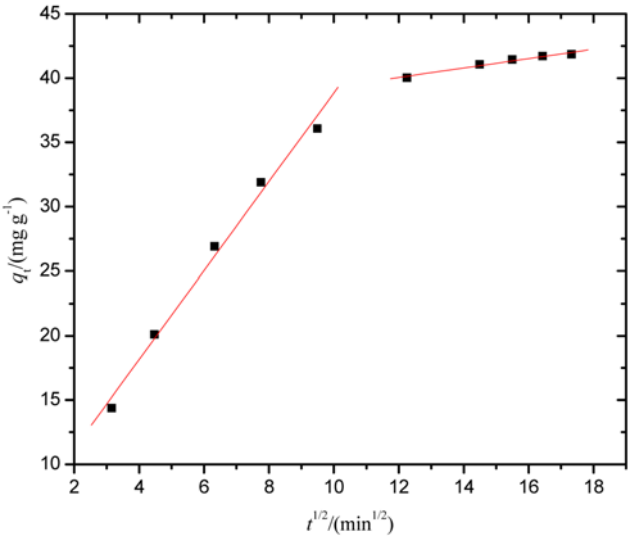

Fig. 14. Intraparticle diffusion plot for adsorption of MB on poplar leaf at 293 K.

second-order model is more close to experimental data. The pseudo first-order model was just applicable for the beginning part of adsorption process. The conclusion expressed that the rate of adsorption process may be controlled by chemical process [32].

Intraparticle diffusion equation is described as

$$q_t = k_i t^{1/2} + C \quad (10)$$

where k_i (mg g^{-1} $min^{-1/2}$) is intraparticle diffusion rate constant, and C is the intercept. The plot of q_t versus $t^{1/2}$ is used to analyze the diffusion mechanism.

The time dependence of q_t in Fig. 14 could be represented in two straight lines which could be well fitted linearly. The multi-linearity relation suggested that the intraparticle diffusion model was dominant in MB adsorption, although the MB adsorption was affected by more than one process [33]. The q_t in the first portion showed a drastic increase with time, which was attributed to the rapid diffusion of dyes through the solution to the external surface of adsorbent. The second portion corresponded to the final equilibration process where the intraparticle diffusion began to slow down. If the lines pass through the origin, then intraparticle diffusion is the only rate controlling step [34]. The two straight lines didn't go through the origin, which suggested that the adsorption process was possibly controlled by some other mechanisms such as the boundary layer effect [12,34].

CONCLUSION

Natural poplar leaf was evaluated as an effective material for MB removal from aqueous solution in batch mode. Adsorptive equilibration could be achieved within 240 min. The amount of dye adsorbed on poplar leaf was influenced substantially by initial pH of dye solution and adsorbent dosage. The salt concentration (Ca^{2+} and Na^{+}) had a negative influence on the dye uptake to some extent. The increasing temperature and dye concentration was favorable for MB removal. MB adsorption on the fallen poplar leaf was found to be a spontaneous and endothermic process according to the thermodynamic study. The adsorption process was found to follow the pseudo second-order kinetics. The intraparticle diffusion model gave two linear regions, which indicated that MB adsorption followed multiple sorption rates. The Langmuir isotherm model well described MB adsorption. The maximum monolayer adsorption capacity determined with the Langmuir model was 135.35 mg g^{-1} at 293 K. The dye-adsorbent interactions were confirmed by FTIR and SEM analysis, and the functional groups such as carboxyl and hydroxyl on the adsorbent surface were responsible for MB adsorption.

ACKNOWLEDGEMENTS

This study was supported by Biochemical Engineering Research Center in Zhengzhou University.

REFERENCES

1. T. Robinson, B. Chandran and P. Nigam, *Water Res.*, **36**, 2824 (2002).
2. Ö. Gerçel, H. F. Gerçel A, Savaş Koparal and Ülker Bakır Öğütveren, *J. Hazard. Mater.*, **160**, 668 (2008).
3. T. Robinson, B. Chandran and P. Nigam, *Bioresour. Technol.*, **85**, 119 (2002).
4. K. V. Kumar and K. Porkodi, *J. Hazard. Mater.*, **146**, 214 (2007).
5. O. Gulnaz, A. Kaya and S. Dincer, *J. Hazard. Mater.*, **B134**, 190 (2006).
6. S. D. Khattri and M. K. Singh, *J. Hazard. Mater.*, **167**, 1089 (2009).
7. A. E. Ofomaja and Y. S. Ho, *Dyes Pigm.*, **74**, 60 (2007).
8. V. Ponnusami, V. Krithika, R. Madhuram and S. N. Srivastava, *J. Hazard. Mater.*, **142**, 397 (2007).
9. T. G Chuah, A. Jumasiah, I. Azni, S. Katayon and S. Y. Thomas Choong, *Desalination*, **175**, 305 (2005).
10. Y. S. Ho, T. H. Chiang and Y. M. Hsueh, *Process Biochem.*, **40**, 119 (2005).
11. K. V. Kumar, *Dyes Pigm.*, **74**, 595 (2007).
12. C. H. Weng, Y. T. Lin and T. W. Tzeng, *J. Hazard. Mater.*, **170**, 417 (2009).
13. M. Dundar, C. Nuhoglu and Y. Nuhoglu, *J. Hazard. Mater.*, **151**, 86 (2008).
14. R. Salim, M. Al-Subu, I. Abu-Shqair and H. Braik, *Inst. Chem. Eng.*, **81B**, 236 (2003).
15. G Bayramöglu and M. Y. Arıca, *J. Hazard. Mater.*, **143**, 135 (2007).

16. T. Akar, I. Tosun, Z. Kaynak, E. Ozkara, O. Yeni, E. N. Sahin and S. T. Akar, *J. Hazard. Mater.*, **166**, 1217 (2009).
17. P. Waranusantigul, P. Pokethitiyook, M. Kruatrachue and E. S. Upatham, *Environ. Pollut.*, **125**, 385 (2003).
18. V. Vadivelan and K. V. Kumar, *J. Colloid Interface Sci.*, **286**, 90 (2005).
19. S. Wang, Z. H. Zhu, A. Coomes, F. Haghseresht and G. Q. Lu, *J. Colloid Interface Sci.*, **284**, 440 (2005).
20. E. Lorenc-Grabowska and G. Gryglewicz, *Dyes Pigm.*, **74**, 34 (2007).
21. R. P. Han, W. H. Zou, W. H. Yu, S. J. Cheng, Y. F. Wang and J. Shi, *J. Hazard. Mater.*, **141**, 156 (2007).
22. R. P. Han, Y. Wang, P. Han, J. Shi, J. Yang and Y. S. Lu, *J. Hazard. Mater.*, **B137**, 550 (2006).
23. Y. Bulut and H. Aydin, *Desalination*, **194**, 259 (2006).
24. K. V. Kumar and A. Kumaran, *Biochem. Eng. J.*, **27**, 83 (2005).
25. Y. Wang, Y. Mu, Q. B. Zhao and H. Q. Yu, *Sep. Purif. Technol.*, **50**, 1 (2006).
26. J. Y. Song, W. H. Zou, Y. Y. Bian, F. Y. Su and R. P. Han, *Desalination*, **265**, 119 (2011).
27. B. Royer, N. F. Cardoso, E. C. Lima, Julio C. P. Vaghetti, N. M. Simon, T. Calvete and R. Cataluna Veses, *J. Hazard. Mater.*, **164**, 1213 (2009).
28. X. L. Han, W. Wang and X. J. Ma, *Chem. Eng. J.*, **171**, 1 (2011).
29. Z. Aksu, *Process Biochem.*, **38**, 89 (2002).
30. G. Annadurai, R.-S. Juang and D.-J. Lee, *J. Hazard. Mater.*, **B92**, 263 (2002).
31. Z. Aksu and G. Karabayır, *Bioresour. Technol.*, **99**, 7730 (2008).
32. Q. L. Fu, Y. L. Deng, H. S. Li, J. Liu, H. Q. Hu, S. W. Chen and T. M. Sa, *Appl. Surf. Sci.*, **255**, 4551 (2009).
33. M. Ugurlu, *Micropor. Mesopor. Mater.*, **119**, 276 (2009).
34. T. Akar, A. S. Ozcan, S. Tunali and A. Ozcan, *Bioresour. Technol.*, **99**, 3057 (2008).
35. M. Dögan, M. Alkan, A. Türkyilmaz and Y. Özdemir, *J. Hazard. Mater.*, **B109**, 141 (2004).